Power Law of Molecular Weight of the Nucleation Rate of Folded Chain Crystals of Polyethylene

Swapan K. Ghosh,[†] Masamichi Hikosaka,*[,†] Akihiko Toda,[†] Shinichi Yamazaki,[†] and Koji Yamada[‡]

Faculty of Integrated Arts and Sciences, Hiroshima University, 1-7-1 Kagamiyama, Higashi-Hiroshima 739-8521, Japan; and Oita Research Center, SunAllomer Limited, Nakanosu, Oita 870-0189, Japan

Received April 4, 2001; Revised Manuscript Received April 16, 2002

ABSTRACT: The molecular weight (M_n) dependence of the primary nucleation rate (I) of folded chain single crystals (FCSCs) of polyethylene (PE) was studied. A power law for the nucleation rate, $I \propto M_n^{-2.4}$, was found. The FCSCs were formed by isothermal crystallization from the melt into an ordered phase (=orthorhombic phase). A new experimental method was established to obtain reliable I, which has been difficult in the case of heterogeneous nucleation for long years. The degree of supercooling (ΔT) dependence of I fits well with the theoretical I given by classical nucleation theory, $I = I_0 \exp(-\Delta G^*/kT) \propto D \exp(-C/\Delta T^2)$, where I_0 is proportional to the topological diffusion coefficient of polymer chains (D), ΔG^* is the free energy for forming a critical nucleus, k is the Boltzmann constant, T is temperature, and C is a constant. It is found that ΔG^* ($\propto C$) does not depend on M_n, while I_0 decreases with increase of M_n, from which it is concluded that formation of a critical nucleus is not controlled by M_n, while only topological diffusion of polymers is controlled by M_n, i.e., $I \propto D(M_n)$. Similar power laws of PE were already found by the present authors on I of extended chain single crystals (ECSCs), i.e., $I \propto M_n^{-1.0}$, and on the lateral growth rates (V) of ECSCs and FCSCs, $V \propto M_n^{-0.7}$ and $V \propto M_n^{-1.7}$, respectively. ECSCs were formed by isothermal crystallization from the melt into a disordered phase (=hexagonal phase). Therefore, it is concluded that a common power law, I, $V \propto D(M_n) \propto M_n^{-H}$ of PE is confirmed, irrespective of nucleation or growth and irrespective of crystalline phases, ordered or disordered phases. It is to be noted that the power H depends on the degree of order of the crystalline phase, from which it is concluded that both nucleation and growth are controlled by the "topological" diffusion of polymer chains within interface between a nucleus (or crystal) and the melt and/or within the nucleus. The "topological" diffusion is related to chain sliding diffusion and disentanglements.

1. Introduction

The primary nucleation mechanism of atomic or low molecular weight systems have been well studied by applying "classical nucleation theory",[1−4] while that of polymers is still an important unsolved problem. In particular, the molecular weight (M_n) dependence of the primary nucleation rate (I) of polymers has remained unsolved for many years, due to experimental difficulties to obtain reliable I and theoretical ones to formulate the "topological nature" of polymer chains. Here M_n indicates the number-averaged molecular weight.

1.1. Power Law of *I* of Extended Chain Single Crystals of Polyethylene. We have recently reported the M_n dependence of I of extended chain single crystals (ECSCs) of polyethylene (PE).[5] ECSCs were crystallized from the melt into the hexagonal phase (=disordered phase) at high pressure where the chain sliding diffusion should be easy.[6,7] It was shown that I satisfies a well-known formula in the classical nucleation theory

$$I = I_0 \exp(-\Delta G^*/kT) = I_0 \exp(-C/\Delta T^2) \qquad (1)$$

where I_0 is so-called prefactor related to the diffusion constant (D), ΔG^* is the free energy necessary for formation of a critical nucleus, k is Boltzmann constant, T is temperature, C is a constant, and ΔT is the degree of supercooling. ΔT is defined by $\Delta T \equiv T_m^0 - T_c$, where T_m^0 is the equilibrium melting temperature and T_c is the crystallization temperature. The important result was that ΔG^* is constant, whereas I_0 decreases with increasing M_n. Therefore, it was concluded that formation process of a critical nucleus does not depend on M_n, while M_n dependence of I is mainly controlled by the "topological diffusion" of polymer chains. An experimental power law

$$I \propto D(M_n) \propto M_n^{-1.0} \qquad (2)$$

was found for the first time. The same power law holds for any ΔT, because C does not depend on ΔT. We have proposed a nucleation model based on the topological diffusion of long polymer chains to explain the experimental results.[5]

Okui et al. also reported the M_n dependence of I of poly(ethylene succinate).[8] They showed that C depends on M_n. In this case, M_n dependence of I depends on ΔT, which is quite different from our results; therefore, they compared Is of different M_ns at different special ΔTs where I shows a maximum. For this reason, although they showed that I increases with increasing molecular weight, which is opposite to our result, it is impossible to compare between us and them.

1.2. M_n Dependence of *I* of Folded Chain Single Crystals of Polyethylene. Recently, we reported preliminary experimental results that I of folded chain single crystals (FCSCs) of PE also shows a similar power law, $I \propto M_n^{-2.3}$.[9] FCSCs were crystallized from the melt into the orthorhombic phase which can be regarded as

* To whom correspondence should be addressed.
[†] Hiroshima University.
[‡] SunAllomer Ltd.

10.1021/ma0105901 CCC: $22.00
Published on Web 07/25/2002

an "ordered phase" where chain sliding should be difficult within a nucleus.[6,7] The preliminary observation was insufficient in obtaining reliable I; therefore it is necessary to obtain a much more reliable I to confirm the power law on FCSCs.

Thus, it was suggested that a common power law for PE may exist, irrespective of crystalline phases, which is expressed by

$$I \propto M_n^{-H} \tag{3}$$

where H is a constant and that the power H depends on the crystalline phases. It should be important to confirm the above suggestion to solve the nucleation mechanism of polymers.

1.3. Difficulties in Obtaining Reliable M_n Dependence of I. It is well-known that the nucleation from the bulky melt is usually a type of "heterogeneous nucleation".[5] In this case, scatter in spatial distribution of the number density of the "heterogeneities" (ν_{het}) is large, which results in large statistical error (ΔI) in I. The surface free energy of the heterogeneities is different for different kind of heterogeneities; therefore ΔG^*, i.e., C, in eq 1 depends on heterogeneities. These two problems are the main difficulties in obtaining reliable M_n dependence of I. The reason why the M_n dependence of I has remained as an unsolved problem for so many years is that it was difficult to overcome the above two difficulties.

In this paper, the two difficulties will be solved by preparing well fractionated samples, which include the same kind of heterogeneity, and by obtaining a significant statistical average of I (I_{av}) from a large number of measurements, and the reliable M_n dependence of I of FCSCs of PE will be confirmed.

1.4. Power Law of the Lateral Growth Rate of ECSC and FCSC of PE. The present authors showed a similar power law for the lateral growth rate (V) of PE[10,11]

$$V \propto D \propto M_n^{-H} \tag{4}$$

where the power $H = 0.7$ for ECSCs formed in the disordered phase and $H = 1.7$ for FCSCs formed in the ordered phase. The results showed that the power H depends on the degree of order of the crystalline phase. Therefore, it was concluded that the $M_n$dependence of V is controlled by the topological diffusion of chains, which acts via chain sliding diffusion and disentanglements, within the interface between the crystal and the melt and/or within the secondary nucleus.

1.5. Purpose of this Study. The purpose of this paper is to confirm the power law of nucleation rate (I) for FCSCs of PE that are formed in the ordered phase from the melt at atmospheric pressure. A reliable method to determine heterogeneous nucleation rate will be established by taking the statistical average of I of the samples with the same kind of heterogeneity. A common power law, I, and V, $I, V \propto D(M_n) \propto M_n^{-H}$, will be proposed, irrespective of crystalline phases and I or V. Physical meaning of the common power law will be discussed using the topological mechanisms of nucleation and growth.

2. Experimental Section

2.1. Sample Preparation. Six samples of PE were fractionated from a single sample (named as the "mother sample") in order to confirm that all samples contain the same type of heterogeneity. The range of M_n was between 13×10^3 and 139×10^3. Number and weight-averaged molecular weights (M_n and M_w) and molecular weight distribution are shown in Table 1. The range of M_n was not wide enough due to experimental difficulties to prepare fractionated samples with the same heterogeneity. But significant M_n dependence of I was obtained in this paper.

Table 1. M_n, M_w, and Molecular Weight Distribution of Polyethylene Fractions Fractionated from a "Mother Sample"

sample name	$M_n/10^3$	$M_w/10^3$	M_n/M_w	T_m^0/°C
J-PE1	13	17	1.28	138.25
J-PE2	30	34	1.15	139.5
J-PE4	50	57	1.14	140.0
J-PE5	71	81	1.14	140.2
J-PE6	99	114	1.14	140.4
J-PE7	139	163	1.17	140.6
mother sample	47.8	116	2.42	

The mother sample was crystallized onto the surface of spherical supports (Celite545) by slow cooling (10 K h^{-1}) from the solution made of a mixed solvent of xylene (good solvent) and ethylene glycol monoethyl ether (poor solvent). It was then dissolved into a mixed solvent, and fractionation was carried out at 400 K by using the column elution method. The ratio of good solvent was increased step by step from 0% to 64%. Fractionated PE was deposited from the fractionated solution at room temperature and was recovered by filtration. The molecular weight was measured by gel permeation chromatography (GPC).

2.2. Equipment and Experimental Conditions. FCSCs were isothermally crystallized from the melt into an ordered (orthorhombic) phase at atmospheric pressure. The range of ΔT was 10−15 K. As mentioned in ref 5, T_c dependence of I was neglected in this paper, because the range of ΔT is small. Samples 0.1 mm thick were put in a hot stage (Linkam, LK-600). The nitrogen gas flow was at a rate of 50 mL/min. Number of isolated crystals near the center of the sample was counted using polarizing optical microscope (Olympus, BX). T_m^0 was determined using Wunderlich's method.[11] The temperature was calibrated using standard materials, In and Sn. To observe isolated single crystals, observation was limited to the earlier stage of crystallization.

2.3. Average of Nucleation Rate, I_{av} and Error. The number density of nuclei, ν increases with the crystallization time, t. I is defined by

$$I \equiv \frac{d\nu}{dt}, \quad \text{for } \nu \ll \nu_{het} \tag{5}$$

where ν_{het} is the number density of active heterogeneity. Number density of the isolated single crystals is assumed to correspond to that of the nuclei, ν. Spatial distribution of ν result in distribution of I, ($f(I)$) which usually involves significant statistical error. The statistical average of I, (I_{av}) was estimated by using the equation

$$I_{av} \equiv \frac{\sum If(I)}{\sum f(I)} \tag{6}$$

ν was observed several times or 10 times at each ΔT. The error in I was evaluated by the standard deviation ΔI. Thus, I was expressed by

$$I = I_{av} \pm \Delta I \tag{7}$$

2.4. Average of Constant C, C_{av}. C corresponds to the slope of straight line of log I vs ΔT^{-2}. Scatter in C cannot be neglected in actual observation, which mainly arises due to the error in ΔT, which is related to uncontrollable factors, such

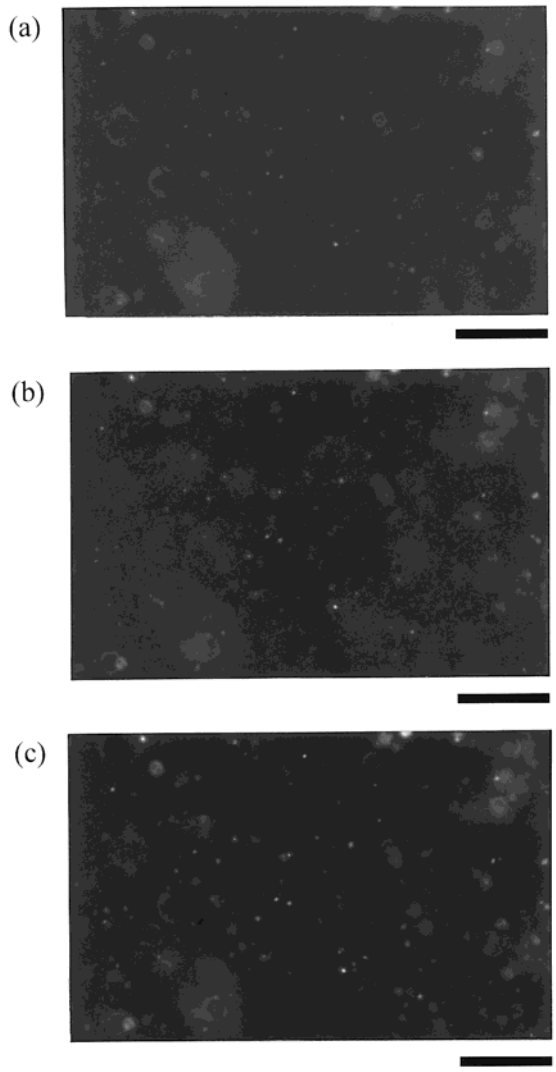

Figure 1. Typical polarizing optical micrographs of growing FCSCs of PE for $M_n = 50 \times 10^3$ at $\Delta T = 12.5$ K: (a) $t = 90$ s, (b) $t = 120$ s, and (c) $t = 135$ s. Scale bar = 50 μm.

as the calibration of temperature, thermal contact between sample and hotstage, fluctuation of the N_2 gas flow in the hotstage, the thickness of the sample, and so on. The statistical average of C was obtained by the equation

$$C_{av} \equiv \frac{\sum Cf(C)}{\sum f(C)} \tag{8}$$

where $f(C)$ is the distribution function of C. The error in C was estimated from the standard deviation, ΔC. Thus, C is expressed by

$$C = C_{av} \pm \Delta C \tag{9}$$

3. Results

3.1. Scatter in *I*. Typical morphology of the crystals and increase of ν with increasing t are shown in Figure 1. ν vs t at $\Delta T = 12.5$ K for all samples are plotted in Figure 2, parts a−e. Thin lines are the best fits for independent measurements. Scatter of ν is clearly observed. τ_{obs} is the average of the observed induction time without correction with respect to growth.

A typical statistical distribution of the nucleation rate $f(I)$ is shown by a histogram in Figure 3 for $M_n = 50 \times 10^3$ at $\Delta T = 12.5$ K. The histogram was fitted by a Gaussian distribution function given by

$$f(I) \propto \exp\{-(I - I_{av})^2/2\Delta I^2\} \tag{10}$$

From Figure 3, I_{av} and ΔI are determined

$$I = I_{av} \pm \Delta I = (1.46 \pm 0.30) \times 10^{-6}\,\mu\mathrm{m}^{-3}\,\mathrm{s}^{-1}, \quad \text{for } M_n = 50 \times 10^3 \tag{11}$$

Therefore, the relative experimental error

$$\Delta I/I_{av} \approx 20\% \tag{12}$$

was shown to be small enough for the present purpose, because it will be shown in section 3.6 that decrease of I with increasing M_n is much larger than ΔI. Similarly, we estimated I_{av}s for other M_ns.

3.2. Scatter in *C*. We have independently measured I vs ΔT^{-2} several times or 10 times for each M_ns (Figure 4, parts a−f). The typical statistical distribution of C, $f(C)$, for $M_n = 139 \times 10^3$ was shown by a histogram in Figure 5. The histogram was fitted by Gaussian distribution function

$$f(C) \propto \exp\{-(C - C_{av})^2/2\Delta C^2\} \tag{13}$$

From Figure 4, C_{av} and ΔC were determined

$$C = C \pm \Delta C = (1.20 \pm 0.14) \times 10^3\ \mathrm{K}^2, \quad \text{for } M_n = 139 \times 10^3 \tag{14}$$

Therefore

$$\Delta C/C_{av} \approx 12\%, \quad \text{for } M_n = 139 \times 10^3 \tag{15}$$

The relative error, $\Delta C/C_{av}$, was again showed to be small enough for the present purpose.

3.3. M_n Dependence of $C \propto \Delta G^*$. C_{av} is plotted against M_n in Figure 6. C_{av} was nearly constant for all M_ns except for $M_n = 13 \times 10^3$.

$$C \cong \text{const} \cong 1.2 \times 10^3\mathrm{K}^2, \quad \text{for } M_n = 30 \times 10^3, 50 \times 10^3, 71 \times 10^3, 99 \times 10^3, \text{ and } 139 \times 10^3 \tag{16}$$

Thus, it is concluded that the above samples contain the same type of active heterogeneity, except for the sample with $M_n = 13 \times 10^3$, which was excluded in this study.

As C_{av} is in proportion to ΔG^*, it is concluded that

$$\Delta G^* \approx \text{const} \tag{17}$$

for all M_ns; i.e., the formation process of a critical nucleus does not depend on M_n.

3.4. log *I* vs ΔT^{-2} using I_{av} and C_{av}. Here, log I vs ΔT^{-2} was plotted using I_{av} and C_{av} in Figure 7 as a parameter of M_n. I is obtained by

$$I = I_0 \exp(-C_{av}/\Delta T^2) \tag{18}$$

and I_0 is obtained by

$$I_0 \equiv \frac{I_{av}(\Delta T)}{\exp(-C_{av}/\Delta T^2)}, \quad \text{for } \Delta T = 12.5\ \mathrm{K} \tag{19}$$

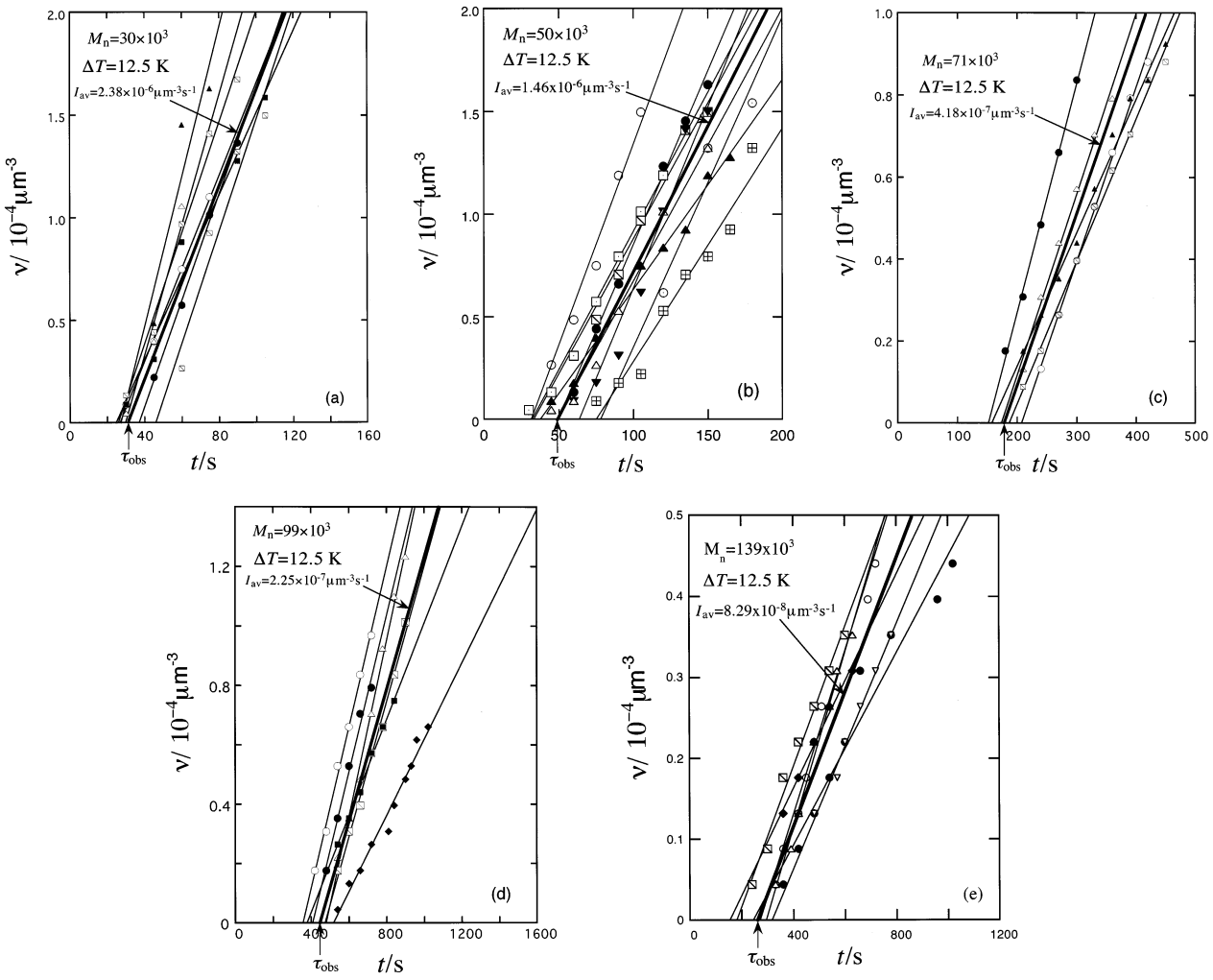

Figure 2. Plots of ν against t at $\Delta T = 12.5$ K: (a) $M_n = 30 \times 10^3$, (b) $M_n = 50 \times 10^3$, (c) $M_n = 71 \times 10^3$, (d) $M_n = 99 \times 10^3$, and (e) $M_n = 139 \times 10^3$. Lines show the best fit of the plots. The slope of each fitting line corresponds to I. Slope of the thick line corresponds to I_{av}. τ_{obs} corresponds to the average observed induction time (without correction of the delay by growth).

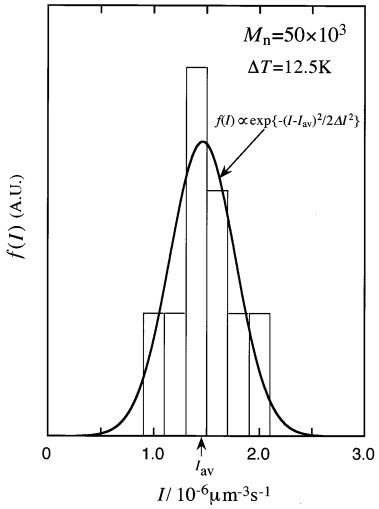

Figure 3. Histogram of typical statistical distribution of I for $M_n = 50 \times 10^3$ at $\Delta T = 12.5$ K. The histogram is approximated by the Gaussian function $f(I)$, shown by the solid curve.

log I decreases significantly with increase of ΔT^{-2} (Figure 7). Each straight line represents different M_n. Hereafter, I and C mean I_{av} and C_{av}, respectively.

3.5. M_n Dependence of I and C. Lines of log I vs ΔT^{-2} in Figure 7 are nearly parallel for all M_ns and they shift downward with increasing M_n. This corresponds to the fact that C does not depend on M_n, while I_0 decreases significantly with increasing M_n. Thus, the observed results can be summarized as follows:

$$I_0 = I_0(M_n) \quad \text{and} \quad C \approx 1.2 \times 10^3\ \text{K}^2 \cong \text{const} \quad (20)$$

This means that only I_0, which is proportional to D, depends on M_n whereas C, which is related to ΔG^*, does not depend on M_n. Equations 2 and 20 yield

$$I(M_n) \propto I_0(M_n) \propto D(M_n) \quad (21)$$

Thus, it is concluded that M_n dependence of I is controlled by the diffusion process of polymer chains and is not controlled by the formation process of a critical nucleus.

3.6. Power Law of Nucleation Rate, I. In Figure 8, log I_0 is plotted against log M_n for the red phase (FCSCs). The fitting lines show the experimental formula. Here, log I_0 decreases linearly with increasing log M_n. Thus, experimental power law

$$I(M_n) \propto I_0(M_n) \propto M_n^{-2.4}, \quad \text{for ordered phase (FCSC)} \quad (22)$$

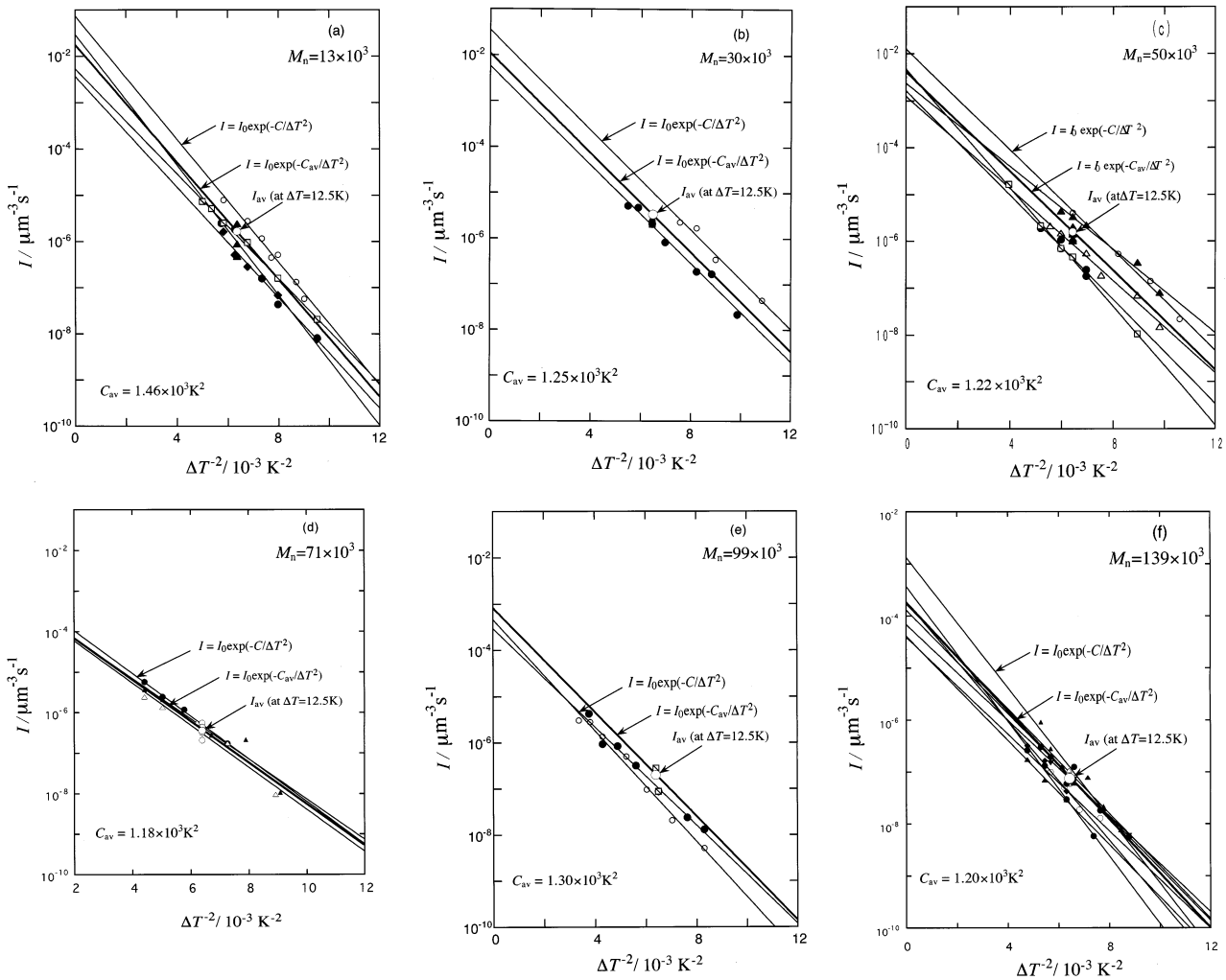

Figure 4. Plots of log I vs ΔT^{-2} for (a) $M_n = 13 \times 10^3$ (b) $M_n = 30 \times 10^3$, (c) $M_n = 50 \times 10^3$, (d) $M_n = 71 \times 10^3$, (e) $M_n = 99 \times 10^3$, and (f) $M_n = 139 \times 10^3$. The solid lines are fitted ones obtained by using the classical nucleation theory (eq 1). C_{av} is the average of C.

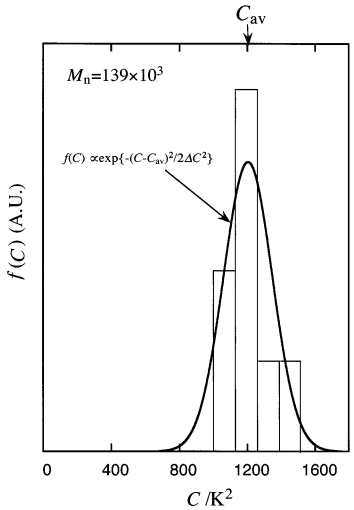

Figure 5. Histogram of typical statistical distribution of C for $M_n = 139 \times 10^3$. The histogram is approximated by the Gaussian function $f(C)$, shown by the solid curve.

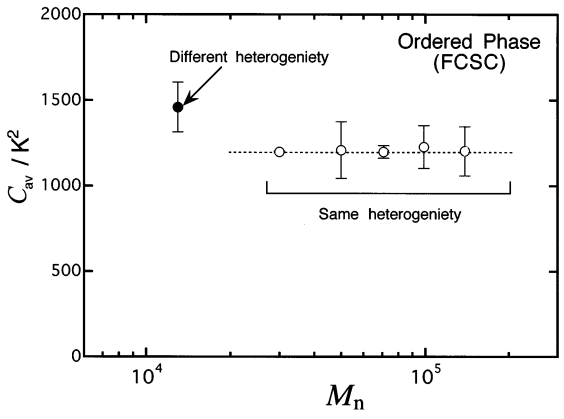

Figure 6. Plots of C_{av} vs log M_n. C_{av} is almost the same for all M_n except for $M_n = 13 \times 10^3$; therefore, it is concluded that the samples except for $M_n = 13 \times 10^3$ contain the same heterogeneity.

is confirmed. Also, log I_0 vs log M_n for the disordered phase (ECSCs) is shown as a reference in Figure 8, which is re-plotted from ref 10. Thus, it is concluded that the power law of I is confirmed both for FCSCs and ECSCs.

4. Discussion

4.1. Power law of *I* and *V*. From this and previous results, a common power law of I and V of PE (Figure 9) is expressed by

$$I,V \propto D(M_n) \propto M_n^{-H} \qquad (23)$$

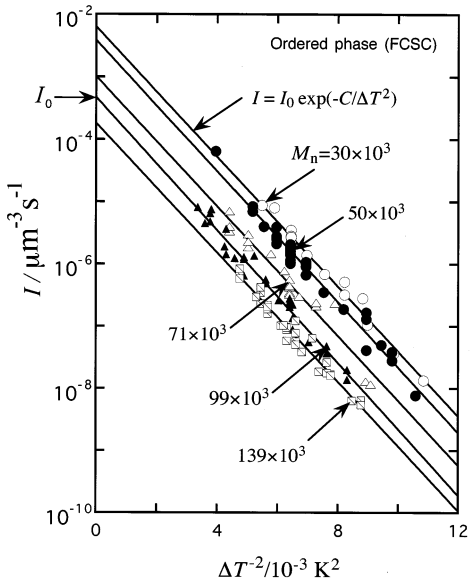

Figure 7. Plot of log I vs ΔT^{-2} for $M_n = 30 \times 10^3$, 50×10^3, 71×10^3, 99×10^3, and 139×10^3. The solid lines represent the best fit of the plots, which corresponds to the classical nucleation theory (eq 1). I_0 is the intercept of the vertical axis at $\Delta T^{-2} = 0$.

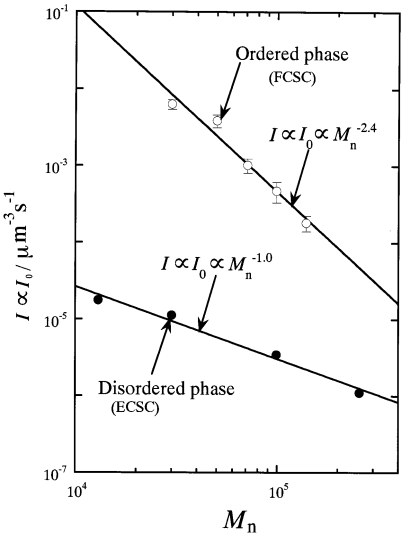

Figure 8. Plot of log I vs log M_n. The best fit line for FCSCs show a power law, $I \propto M_n^{-2.4}$. The result for ECSCs is re-plotted for comparison from ref 10.

where H is summarized for I

$$\begin{aligned} H &= 2.4 \quad \text{ordered phase (FCSC)} \\ &= 1.0 \quad \text{disordered phase (ECSC),} \end{aligned} \tag{24}$$

and for V

$$\begin{aligned} H &= 1.7 \quad \text{ordered phase (FCSC)} \\ &= 0.7 \quad \text{disordered phase (ECSC)} \end{aligned} \tag{25}$$

It is concluded that H increases with the increase of degree of order of the crystalline phases

$$H(\text{ordered}) > H(\text{disordered}) \tag{26}$$

It is also concluded that H of I is larger than that of V

$$H(I) > H(V) \tag{27}$$

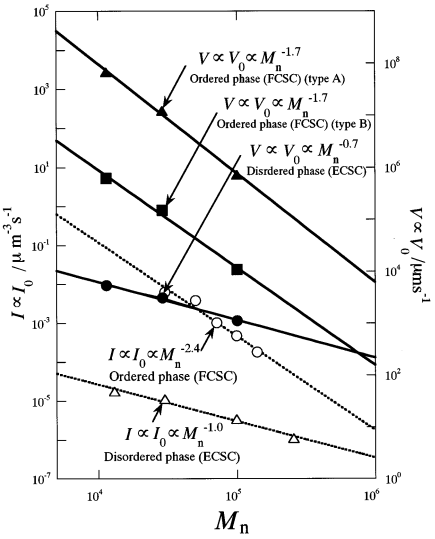

Figure 9. Plot of log I and log V against log M_n for ordered and disordered phases where FCCs and ECCs are formed, respectively, from which a common power law of I and V for PE, $I,V \propto D(M_n) \propto M_n^{-H}$, is proposed. Solid and broken lines are the best-fit lines of the experimental power laws. It is to be noted that H of the ordered phase is larger than that of the disordered one.

The physical meaning of this will be discussed in the next section.

4.2. Crystalline Phase Dependence of *H*: Experimental Evidence of Chain Sliding Diffusion. It is important to consider why H depends on the degree of order of the crystalline phase. Three different types of diffusion process may act during the process of nucleation and growth. They are diffusion within the melt, within the interface between the melt and a nucleus (or crystal), and within the nucleus. It is obvious that the diffusion of chains within the melt is not related with the dependence of H on the degree of order of the crystalline phase within the nucleus (or crystal). Therefore, phase dependence of H should arise from the diffusion of chains within the interface between the melt and nucleus (or crystal) and/or in nucleus. These diffusions are the chain sliding diffusion along the chain axis.

Thus, the phase dependence of H should be experimental evidence that sliding diffusion (within the interface between the melt and nucleus or crystal and within the crystalline phase) takes important role in the nucleation and growth mechanisms. It is obvious that the chain sliding diffusion is sensitive to the degree of order of the crystalline phase.

4.3. Comparison of the Experimental Facts with the Sliding Diffusion Theory of Nucleation. The observed power law can be well explained by the chain sliding diffusion theory of nucleation proposed in the previous paper.[10] The theory formulated

$$I \propto D(M_n) \propto M_n^{1-3\alpha} \tag{28}$$

where α is a kind of order parameter related to the degree of order of the crystalline phase. Correspondence of the experimental formula (eq 23) and theoretical formula (eq 28) yields

$$H = 3\alpha - 1 \tag{29}$$

For I, comparison of (24) and (29) yields

$$\begin{aligned} \alpha &= 1.13 \quad \text{ordered phase} \\ &= 0.66 \quad \text{disordered phase} \end{aligned} \tag{30}$$

For V, comparison of (25) and (29) yields

$$\begin{aligned} \alpha &= 0.93 \quad \text{ordered phase} \\ &= 0.56 \quad \text{disordered phase} \end{aligned} \tag{31}$$

Equations 30 and 31 show that for both I and V

$$\alpha(\text{ordered phase}) > \alpha\,(\text{disordered phase}) \tag{32}$$

α for the ordered phase is twice as large as that for the disordered phase. Since α is a kind of order parameter which should relate to the degree of order of the crystalline phase, the result of eq 32 is reasonable. Therefore, it is shown that the topological model is reasonable.

5. Conclusion

1. A reliable method is established to determine the molecular weight M_n dependence of the heterogeneous primary nucleation rate I by taking a statistical average of I. The method was applied to the nucleation of folded chain crystals (FCCs) of polyethylene (PE) formed from the melt into the orthorhombic phase, which can be regarded as the "ordered phase".

2. The free energy necessary for the formation of a critical nucleus ΔG^* does not depend on M_n, i.e., $\Delta G^* \approx$ const, while the diffusion coefficient D does depend on M_n, i.e., $I \propto I_0(M_n) \propto D(M_n)$. Therefore, the M_n dependence of I is not controlled by the formation process of a critical nucleus and is mainly controlled by the diffusion process.

3. A power law of nucleation rate, $I \propto M_n^{-2.4}$ was confirmed for nucleation from the melt into the "ordered phase" where FCC is formed.

4. By combination of the present results with previous ones, a "common power law" for the primary nucleation and growth rates of PE, $I,V \propto D(M_n) \propto M_n^{-H}$ was proposed, where H is a constant. H increases with the increase of the degree of order of the crystalline phase from the hexagonal to the orthorhombic phases.

5. A topological model is proposed where the nucleation and growth processes are controlled by the chain sliding diffusion and the disentanglement ones within the interface between a nucleus (or crystal) and the melt and/or within the nucleus.

Acknowledgment. The authors gratefully acknowledge the financial support provided by the Grant in Aid for Scientific Research on Priority Areas B2 (No. 12127205), Scientific Research A2 (No. 12305062), Scientific Research C2 (No. 11640378), and Grant in Aid for JSPS Fellows (No.10098434-00).

References and Notes

(1) Becker, V. R.; Döring, W. *Ann. Phys. (Berlin)* **1935**, *24*, 719.
(2) Turnbull, D.; Fisher, J. C. *J. Chem. Phys.* **1949**, *17*, 71.
(3) Frank, F. C.; Tosi, M. *Proc. R. Soc.* **1961**, *A263*, 323.
(4) Price, F. P. Nucleation in polymer crystallization. In *Nucleation*; Zettlemoyer, A. C., Ed.; Marcel Dekker: New York, 1969; pp 405−488.
(5) Nishi, M.; Hikosaka, M.; Ghosh, S. K.; Toda, A.; Yamada, K. *Polym. J.* **1999**, *31*, 749.
(6) Hikosaka, M. *Polymer* **1987**, *28*, 1257.
(7) Hikosaka, M. *Polymer* **1990**, *31*, 458.
(8) Umemoto, S.; Hayashi, R.; Okui, N. To be published.
(9) Ghosh, S. K.; Hikosaka, M.; Toda, A. *Colloid Polym. Sci.* **2001**, *279*, 382.
(10) Nishi, M.; Hikosaka, M.; Toda, A.; Takahashi, M. *Polymer* **1998**, *39*, 1591.
(11) Okada, M.; Nishi, M.; Takahashi, M.; Matsuda, H.; Toda, A.; Hikosaka, M. *Polymer* **1998**, *39*, 4535.

MA0105901